X-Ray Photoelectron Diffraction (XPED) Studies on Metal Oxide Surfaces. (I) Analysis of the XPED Patterns from TiO_2(001) and α-Al_2O_3(0001) by the Single Scattering Calculation

Koji TAMURA,* Masanori OWARI, Masahiro KUDO, and Yoshimasa NIHEI
Institute of Industrial Science, University of Tokyo,
7-22-1 Roppongi, Minato-ku, Tokyo 106
(Received January 5, 1985)

X-Ray photoelectron diffraction (XPED) measurements were applied to the (001) surface of TiO_2 rutile and the (0001) surface of α-Al_2O_3 in order to examine the applicability of XPED to metal oxides. Obtained XPED patterns were compared with the results of theoretical calculations based on a single scattering model. The calculated patterns from both oxides agreed with the experimental patterns. It was revealed from theoretical calculations that the four oxygen atoms in the unit cell of TiO_2 made different contributions to the XPED pattern which reflected different atomic environments. The same calculation was also made on titanium in TiO_2, and on aluminum and oxygen in Al_2O_3. This clarified the contributions of nonequivalent sites of emitter atoms to the main peaks in the experimental XPED patterns. In comparison with the crystal structures, some peaks could be attributed to some specific emitters or specific emitter-scatterer pairs. This analysis was found to be useful to interpret experimental XPED patterns, and is expected to be applied to the analysis of the structures of surfaces or interfaces related to such phenomena as selective desorption or substitution of specific site of atoms.

It is known that angular distributions of XPS intensities from single crystals exhibit fine structures [1—4]. This modulation of photoelectron intensities is caused by the diffraction effect of photoelectrons excited in a single crystal by X-ray radiation, and is called X-ray photoelectron diffraction (XPED). Since XPED patterns reflect atomic arrangements, structural information regarding material can be obtained from an XPED measurement. The information derived from an XPED measurement can be summarized as 1) symmetry and orientation of the crystal surface [5,6], 2) atomic sites in the crystal [7—12], 3) crystal regularity [5,13], and 4) adsorption structure [14—16]. The influence of crystal symmetry and orientation on the XPED patterns have been investigated in detail by the present authors using GaAs(110) and Ge(110) [6]. The knowledge obtained in that study was then used to characterize such systems as the epitaxially grown Au overlayers on the GaAs(110) surface [5].

The XPED studies on a compound mixed crystal $Ga_{1-x}Al_xAs$ [9] showed correspondence between XPED patterns and the sites of photoelectron emitter atoms in the crystal, which indicated that XPED patterns can be regarded as finger prints of atomic sites. This method, therefore, can be used to determine the atomic sites of the foreign atoms in the crystal surface layers [11,12]. In the case of Au/GaSb interface [7], it was concluded that gold atoms occupy the equivalent atomic sites to gallium atoms.

XPED can further be used to estimate the crystal structural regularity. For example, measurements on the ion-bombarded GaAs(110) surface [5] made it possible to evaluate the crystal regularity and the thickness of the disordered layers in the surface region.

XPED can also provide information about the adsorption structure on the surface. The adsorption site of oxygen on the O/c(2×2)Cu(001) [14,15] and the bond orientation of adsorbed CO on the CO/Ni-(001) [16] have been reported.

The purpose of this study is to apply XPED to metal oxides and to investigate their surface structures. Metal oxides are used in many fields as solar cells, sensors, electronic devices, catalysts, absorbents and substrates for crystal growth. It is, therefore, very important to sufficiently characterize the surface structure and the chemical state of the oxide in order to control and reproduce their properties.

In general, in order to obtain structural information regarding the crystal surface, low energy electron diffraction (LEED) or reflection high energy electron diffraction (RHEED) have been used. However, in the case of the metal oxide, these conventional diffraction methods cannot be effectively used due to several reasons. First, they cannot distinguish the contribution from each component. This means that they are not suitable for the analysis of the complicated changes which occur on such samples as metal oxides. Secondly, these metal oxides suffer from severe charge-up problems because of irradiation of high-density primary electron beams. Thirdly, they generally require rather long-range ordering to obtain explicit diffraction patterns.

On the other hand, XPED does not have these drawbacks. Therefore, it can be expected that by using this new method, useful information can be provided regarding the surface structures of metal oxides.

In this study, the XPED patterns for metal oxides were obtained and compared with the results of theoretical calculations. The metal oxides selected for this study were the (001) surface of TiO_2 rutile and the (0001) surface of α-Al_2O_3, which are of great importance in connection with catalysts and have been investigated by many other methods [17—19].

Experimental

Apparatus. All experiments were performed with an angle-resolved X-ray photoelectron spectrometer [6,20] with an aperture in front of the entrance lens of the hemispherical analyzer in order to restrict the solid angle of photoelectron detection. The position-sensitive detection system compensates for the reduced photoelectron intensity due to the restriction of the solid angle. The angular scans were automatically performed using a two-axis sample rotation manipulator. The direction of the normal of the surface was defined as a polar angle of θ=0°, and the direction parallel to the surface was θ=90° [10]. The mean divergence of the acceptance angle was 1.3° along the polar-angle scan and 2.0° perpendicular to the polar-angle scan. The pressure during all measurements was kept below 5×10^{-9} Torr†. Al $K\alpha$ radiation was used to excite photoelectrons.

Samples. A (001) oriented TiO_2 single crystal (10×10×1 mm; Murakami Engineering Co. Ltd) was mechanically polished using a diamond polishing powder. A (0001) oriented Al_2O_3 single crystal (8×9×0.5 mm; Kyoto Ceramic Co. Ltd) had been polished beforehand. Both samples were chemically etched in HCl and in NaOH, and were thoroughly rinsed with distilled water. Before measurements, both samples were annealed in vacuum at 773 K for 50 min and at 823 K for 20 min, respectively, to reduce contaminations. It was confirmed by XPS that there were no carbon nor other impurities after the surface cleaning. Although a slight charge-up effect was observed on both samples, it did not cause any problems on the XPS spectrum shape and intensity.

Results and Discussion

TiO_2(001). (a) XPED Patterns from Oxygen Atoms: The azimuthal dependences of O1s emission from TiO_2(001) are shown in Fig. 1(a). The crystal structure of TiO_2 rutile [21] is also shown as the inset in Fig. 1. The polar angle θ=39° was chosen since the preliminary polar dependence measurement at ϕ=45° showed an intensity maximum at around θ=39°. As for the azimuthal angle, ϕ=0° is defined on the (010) plane and was determined by considering the symmetry property of the crystal. As can be seen in this XPED pattern, the photoelectron intensity maxima were observed at ϕ=0° (This angle is equivalent to 90° by the symmetry of the crystal.) and at ϕ=45°. The peaks at ϕ=45° are relatively sharp, whereas the peaks at ϕ=0° and 90° are broad. The results of the theoretical calculations based on the single scattering model [22] are also shown in Fig. 1(b) as a comparison with those obtained from the experiments. Although the relative intensities of peaks are somewhat different, the calculated XPED pattern reproduces the features of the experimental XPED pattern very well.

There are four kinds of atomic sites which are occupied by oxygen atoms in the unit cell of the TiO_2 crystal, as is shown in Fig. 1. Generally, the atomic arrangements surrounding these oxygen atoms are not equivalent to each other on the occasion of the photoelectron diffraction, though

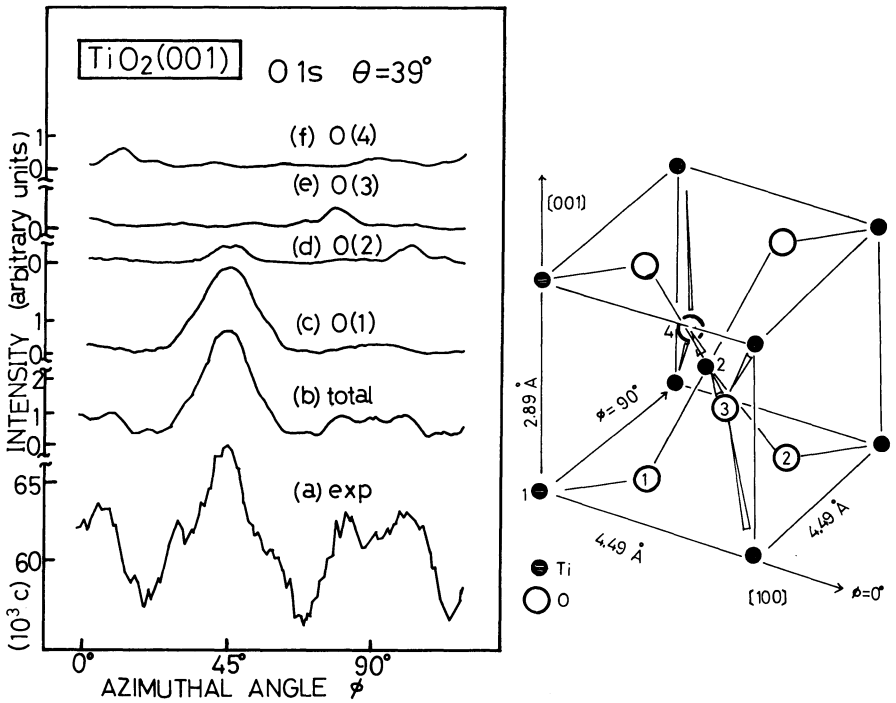

Fig. 1. XPED patterns of O1s from TiO_2(001) and crystal structure. (a) Experimental pattern. (b) Total calculated pattern. (c)—(f) Calculated patterns for each site of oxygen atom.

† 1 Torr ≈ 133.322 Pa.

these four sites become equivalent by rotating the arrangements by some multiples of 90°. As an XPED pattern is known to vary according to the environment of the photoelectron emitter atom, each XPED pattern from nonequivalent atomic sites should be different. An experimentally observed pattern is regarded as the sum of each pattern, and the contribution of each site can not be decomposed. On the other hand, in the theoretical calculation, XPED patterns from these four atomic sites can be individually obtained. The calculated XPED patterns from oxygen atoms in the different sites are shown in Fig. 1 (c—f). The four oxygen atomic sites O(1)—O(4) indicated for each pattern correspond to those shown in the crystal structure.

By comparing the individual calculated patterns with the total calculated pattern (b), it is easily understood that the peak at an azimuthal angle ϕ=45° is mainly due to the photoelectrons from oxygen atom O(1) and slightly to those from the oxygen atom O(2), and also understood that no contribution is made by the oxygen atom O(3) or O(4) at this angle. A similar comparison is also possible for other peaks. The peak at ϕ=12° was revealed to be constructed due to the contribution of oxygen atom O(4), and the peak at ϕ=78° by oxygen atom O(3).

The peak at ϕ=45° will be discussed in more detail in order to understand the origin of this peak. It is known that strongly peaked forward scattering is dominant in the scattering of electrons in metals with kinetic energies about 1000 eV [23,24]. The cause for this effect is that the magnitude of the atomic-scattering factor $f_j(\theta_j)$ is very strongly peaked in the forward direction, and that in this direction the scattering phase shift is rather small. The calculated polar dependence of Ols emission from oxygen atom O(1) at ϕ=45° showed an intensity maximum at θ=39°. This direction (θ,ϕ)=(39°,45°) is almost the same as that of the vector O(1)→Ti(2) in TiO_2. Taking all these facts into account, it is concluded that the experimental peak at ϕ=45° in the azimuthal pattern (Fig. 1(a)) originates mainly from the forward scattering of photoelectrons from the oxygen atom O(1) by the titanium atom Ti(2).

(b) XPED Patterns from Titanium Atoms: In Fig. 2 the azimuthal dependences of Ti2p emission at polar angle θ=39° are shown for TiO_2(001). As is seen in the experimentally obtained XPED pattern (Fig. 2 (a)), there are sharp and strong peaks at ϕ=0° and ϕ=±45°. The results of calculations are also shown in Fig. 2 (b) and they reproduce the features and the relative intensities of the experimental XPED patterns very well. In a TiO_2 crystal, these are two nonequivalent Ti atomic sites as are shown in Fig. 1. The calculated XPED patterns for each site of titanium atom are also shown in Fig. 2 (c—d). It is evident from these results that both emitter atoms Ti(1) and Ti(2) significantly contribute to all of the main peaks at ϕ=0° and ϕ=±45°, which is different

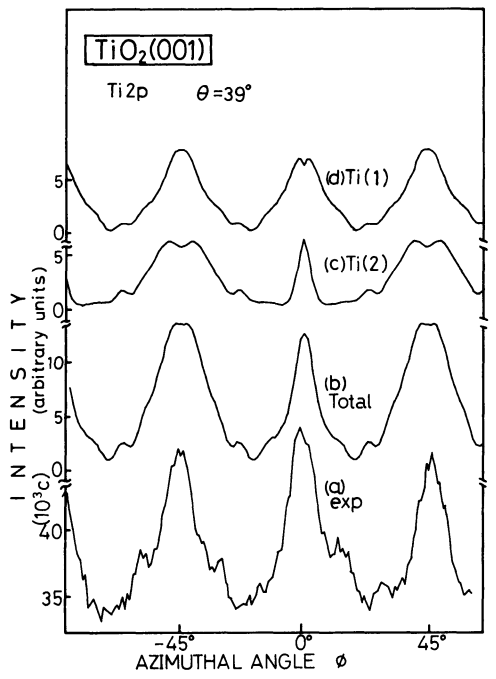

Fig. 2. XPED patterns of Ti2p from TiO_2(001). (a) Experimental pattern. (b) Total calculated pattern. (c), (d) Calculated patterns for each site of titanium atom.

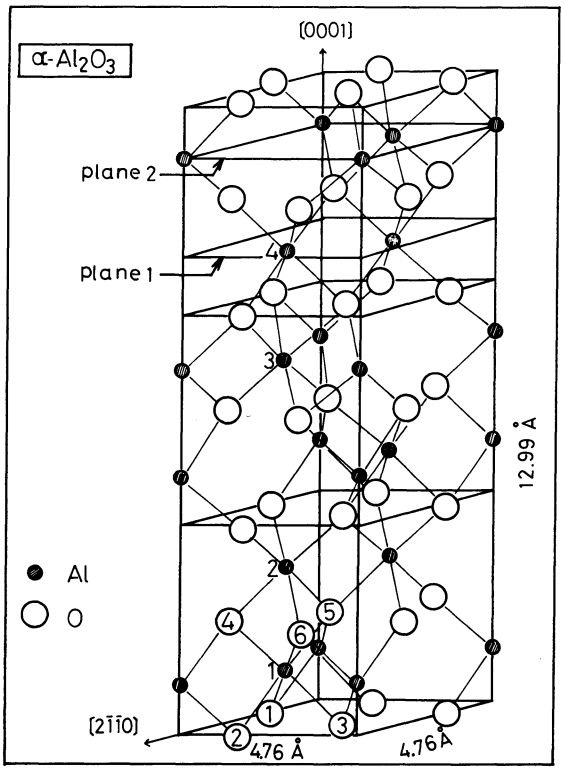

Fig. 3. Crystal structure model of α-Al_2O_3.

from the case of oxygen.

Al_2O_3(0001). (a) XPED Patterns from Aluminum Atoms: The crystal structure of α-Al_2O_3 is shown in Fig. 3. The atomic positions of aluminum atoms and oxygen atoms in the hexagonal unit cell of α-Al_2O_3 were calculated from the results of X-ray diffraction measurement [25]. In an α-Al_2O_3 crystal, aluminum atoms are displaced about 0.2 Å upward or downward from the ideal plane along the c-axis. This displacement was taken into account in the theoretical calculation. On the other hand, the displacement of oxygen atoms in the c-plane was neglected. The azimuthal dependences of Al2s emission at polar angle θ=50° relative to surface normal are shown in Fig. 4. In the experimental XPED pattern (a), there are six peaks at −90°, −60°, −30°, 0°, 30°, 60°, whose shapes and relative intensities are not equal each other. Because of the symmetry of the crystal, ϕ=−90° is equivalent to ϕ=30°. In this figure, azimuthal angle ϕ=0° was on the (01$\bar{1}$0) plane of the hexagonal system. The result of the theoretical calculations is also shown in Fig. 4 (b). Though only single scattering was taken into account, the calculated results agreed well with the experimental results.

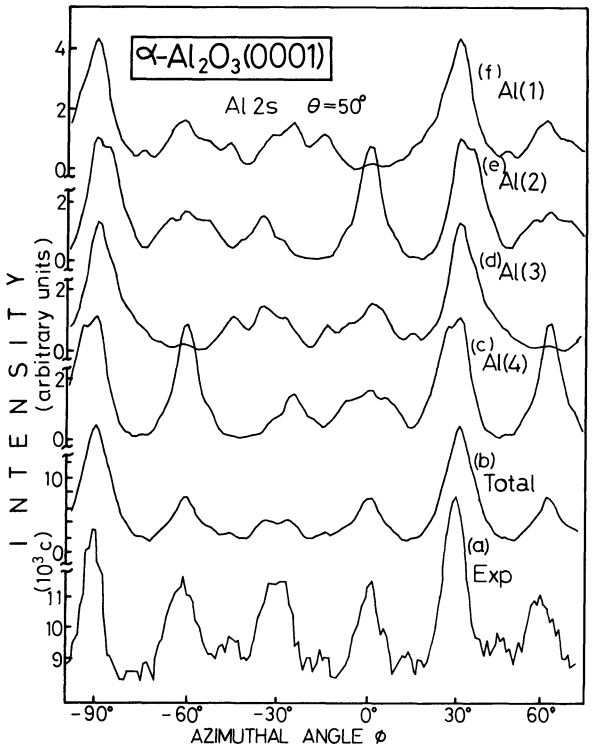

Fig. 4. XPED patterns of Al2s from α-Al_2O_3(0001). (a) Experimental pattern. (b) Total calculated pattern. (c)—(f) Calculated patterns for each site of aluminum atom.

There are four nonequivalent Al atomic sites in an α-Al_2O_3 crystal which are denoted as Al(1)—Al(4) as are shown in Fig. 3. Calculated XPED patterns for these four aluminum atoms are shown as Fig. 4(c)—(f), respectively. By comparing these calculated XPED patterns with the experimental pattern, it is easily seen how each peak in the experimental XPED pattern is constructed. The peak at ϕ=30° is constructed by the contribution of all four emitter atoms and this peak becomes rather a strong one. On the other hand, the peak at ϕ=0° is constructed mainly by the contribution of emitter atom Al(2) and the peak at ϕ=−60° is constructed mainly by the contribution of emitter atom Al(4), and these two peaks become relatively weak.

It is interesting to note the peak at ϕ=−30°. The

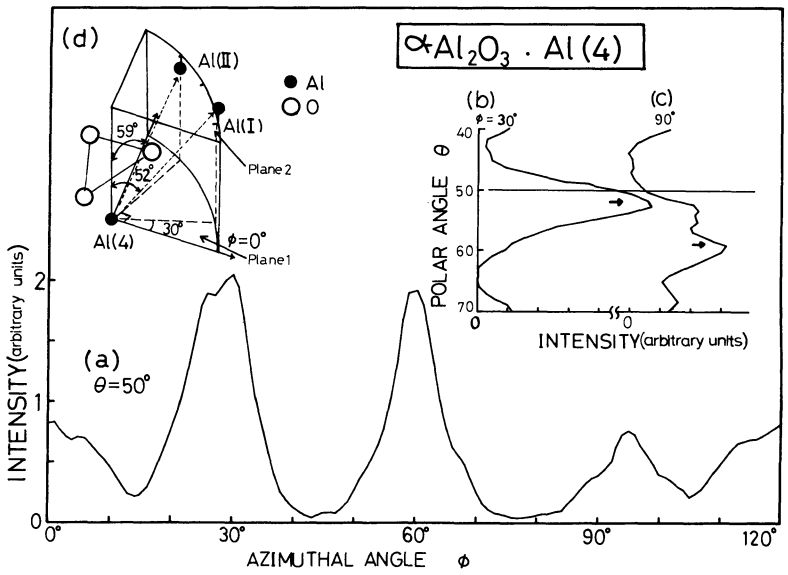

Fig. 5. XPED patterns calculated for aluminum atom Al(4) in α-Al_2O_3. (a) Azimuthal dependences. (b), (c) Polar dependences. (d) Atomic arrangement.

experimentally obtained peak is symmetrical and the top of the peak is flat. The comparison with each calculated pattern revealed that all four emitter atoms contribute to this peak and that the peak positions of each pattern deviated from $\phi=-30°$ to a higher or lower azimuthal angle. The peak shapes of patterns due to aluminum atoms Al(1) and Al(3) or due to aluminum atoms Al(2) and Al(4) are in the relation of a mirror symmetry about $\phi=-30°$. Thus, the total shape of these four patterns becomes a symmetrical one.

The relation between the direction from the emitter atom to the scatterer atom and the XPED pattern is discussed below by use of aluminum atom Al(4) (as an example). Figure 5 shows the calculated results for aluminum atom Al(4) and its atomic environment. The bottom curve (a) shows the azimuthal dependence at $\theta=50°$, and in the upper right, the polar dependences at some azimuthal angles are shown (b—c). In the same figure, some of the surrounding atoms of the emitter atom are also illustrated (d) where the emitter atom Al(4) is on a plane 1, and the scatterer atoms Al(I) and Al(II) are located almost on a plane 2. More strictly, the aluminum atom Al(I) displaces upward and Al(II) downward from a plane 2, as was mentioned before (also see Fig. 3). In the azimuthal dependence (a), there is a strong peak at $\phi=30°$, and this azimuthal

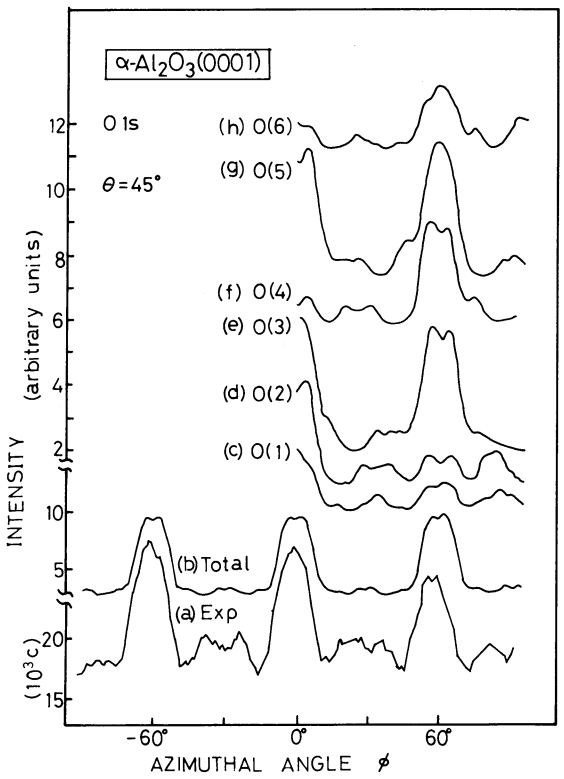

Fig. 6. XPED patterns of O1s from α-Al_2O_3 (0001). (a) Experimental pattern. (b) Total calculated pattern. (c)—(h) Calculated patterns for each site of oxygen atom.

direction is the direction from emitter atom Al(4) to the scatterer atom Al(I). The polar dependence at $\phi=30°$ (Fig. 5(b)) shows the peak at $\theta=52°$. This direction $(\theta,\phi)=(52°,30°)$ coincides with the direction from emitter Al(4) to scatterer Al(I). From this fact, the peak in curve (a) at $\phi=30°$ can be attributed to the forward-scattering peak by the emitter Al(4) and the scatterer Al(I).

On the other hand the shoulder at $\phi=90°$ in curve (a) has a different character. As shown in (d), the azimuthal angle $\phi=90°$ corresponds to the direction from Al(4) to Al(II). The polar angle of this direction is 59°, which leads to the appearance of a peak at $\theta=59°$ in the polar dependence curve (c). From this analysis it is understood that the small hump at $\phi=90°$ in the curve (a) at $\theta=50°$ is just the skirt of the forward-scattering peak which arises from the combination of the emitter Al(4) and the scatterer Al(II).

(b) XPED Patterns from Oxygen Atoms: Azimuthal dependences of Ols emission from α-Al_2O(0001) at polar angle $\theta=45°$ are shown in Fig. 6. As seen in this figure, strong peaks were found at $\phi=0°$, and $\phi=\pm60°$. The results of the theoretical calculations are also shown in Fig. 6(b). The comparison between these results showed that each main peak in the experimental pattern was reproduced by theoretical calculations. For the oxygen atoms in an α-Al_2O_3 crystal, there are six nonequivalent atomic sites, and these six atomic sites O(1)—O(6) correspond to those shown in Fig. 3. The calculated patterns obtained from each emitter atom O(1)—O(6) are shown in Fig. 6(c—h). It is evident that the main peaks in the experimental pattern are constructed by the contributions of some specific emitters.

As shown above, clear XPED patterns for the constituent elements on the metal oxide surfaces were obtained on which structural analysis is generally not easy because of the charge-up problem. A calculation based on the single scattering model explains the experimental results. It is found that the comparison of the total XPED pattern with each pattern from nonequivalent sites of atoms clarified the origin of XPED patterns. Therefore, such a comparison is useful in interpreting the experimental XPED patterns, and some main peaks were, for example, interpreted as the forward-scattering peaks from a specific emitter atoms by the surrounding scatterer atoms. When selective substitution or desorption takes place, some of the peaks in the experimental XPED patterns which are related to the specific sites of atoms appear and/or disappear. It is expected that the XPED analysis can be applied to the characterization of the surface or interface resulting from the reaction on the metal oxide surface. This is very difficult or impossible to be analyzed by other techniques.

References

1) K. Siegbahn, U. Gelius, H. Siegbahn, and E. Olson, *Phys. Scr.*, **1**, 272 (1970).
2) C. S. Fadley and S. Å. L. Bergström, *Phys. Lett. A*, **35**, 375 (1971).
3) J. Brunner and M. Thüler, *Helv. Phys. Acta*, **51**, 21 (1978).
4) M. Kudo, M. Owari, Y. Nihei, Y. Gohshi, and H. Kamada, *Jpn. J. Appl. Phys.*, **17**, Suppl. 17-2, 275 (1978).
5) M. Kudo, N. Koshizaki, M. Owari, Y. Nihei, and H. Kamada, *Hyoumen Kagaku*, **1**, 48 (1980).
6) M. Owari, M. Kudo, and Y. Nihei, *J. Electron Spectrosc.*, **22**, 131 (1981).
7) N. Koshizaki, M. Kudo, M. Owari, Y. Nihei, and H. Kamada, *Jpn. J. Appl. Phys*, **19**, L349 (1980).
8) Y. Nihei, M. Owari, N. Koshizaki, M. Kudo, and H. Kamada, *Proc. Japan Acad.*, **56B**, 654 (1980).
9) Y. Nihei, M. Owari, M. Kudo, and H. Kamada, *Jpn. J. Appl. Phys.*, **20**, L420 (1981).
10) M. Owari, P.-X. Jien, M. Kudo, Y. Nihei, and H. Kamada, *Bunko Kenkyu*, **32**, 103 (1983).
11) J. M. Adams, S. Evans, and J. M. Thomas, *J. Am. Chem. Soc.*, **100**, 3260 (1978).
12) S. Evans, E. Raftery, and J. M. Thomas, *Surf. Sci.*, **89**, 64 (1979).
13) M. Owari, M. Kudo, Y. Nihei, and H. Kamada, *Jpn., J. Appl. Phys.*, **19**, 1203 (1980).
14) S. Kono, C. S. Fadley, N. F. T. Hall, and Z. Hussain, *Phys. Rev. Lett.*, **41**, 117 (1978).
15) S. Kono, S. M. Goldberg, N. F. T. Hall, and C. S. Fadley, *Phys. Rev. Lett*, **41**, 1831 (1978).
16) L. G. Petersson, S. Kono, N. F. T. Hall, C. S. Fadley, and J. B. Pendry, *Phys. Rev. Lett.*, **42**, 1545 (1979).
17) C. C. Change, *J. Appl. Phys.*, **39**, 5570 (1968).
18) T. M. French and G. A. Somorijai, *J. Phys. Chem.*, **74**, (1979).
19) R. H. Tait and R. V. Kasowski, *Phys. Rev. B*, **20**, 5178 (1979).
20) M. Kudo, Y. Nihei, and H. Kamada, *Rev. Sci. Instrum.*, **49**, 756 (1978).
21) W. G. Wyckoff, "Crystal Structures," Interscience Publishers Inc., New York (1948), Chap. IV p5.
22) M. Owari, M. Kudo, Y. Nihei, and H. Kamada, *J. Electron Spectrosc. Relat. Phenom.*, **34**, 215 (1984).
23) S. Kono, S. M. Goldberg, N. F. T. Hall, and C. S. Fadley, *Phys. Rev. B*, **22**, 6085 (1980).
24) J. B. Pendry, "Low Energy Electron Diffraction," Academic, London (1974), Chap. 2.
25) R. E. Newnham and Y. M. De. Haan, *Z. Krist.*, **117**, 235 (1962).